Applied Catalysis B: Environmental 144 (2014) 750–759

Contents lists available at ScienceDirect

Applied Catalysis B: Environmental

journal homepage: www.elsevier.com/locate/apcatb

Atomic level characterization and sulfur resistance of unsupported W_2C during dibenzothiophene hydrodesulfurization. Classical kinetic simulation of the reaction

Marek Lewandowski[a,*], Agnieszka Szymańska-Kolasa[b], Céline Sayag[c], Patricia Beaunier[c], Gérald Djéga-Mariadassou[d,1]

[a] Centre of Polymer and Carbon Materials, Marii Curie Skłodowskiej 34, 41-819 Zabrze, Poland
[b] Johnson Matthey plc, Emission Control Technologies, Orchard Road, Royston, Hertfordshire SG85HE, UK
[c] Laboratoire Réactivité de Surface, UPMC Université Paris 6, UMR 7197-CNRS, 3 rue Galilée, 94200 Ivry, France
[d] UPMC, France

ARTICLE INFO

Article history:
Received 16 April 2013
Received in revised form 6 August 2013
Accepted 7 August 2013
Available online 21 August 2013

Keywords:
W_2C
DBT HDS
5 days of HDS runs
Adsorbed sulfur species
Two kinds of sites

ABSTRACT

The stability of unsupported W_2C tungsten carbide and its sulfur resistance during hydrodesulfurization (HDS) of dibenzothiophene (DBT) are a specificity of W_2C. This material was characterized by X-ray diffraction, specific surface area measurements, HRTEM associated with EDS, lattice images, direct and reverse Fast Fourier Transforms, direct lattice fringes profiles, dynamic CO chemisorptions and elemental analysis of S, C and W. The absence of surface crystallographic layer of tungsten sulfide and the presence of a surface monolayer of "adsorbed sulfur species" (post-sulfur passivation by H_2S by the end of HDS runs), after 5 days of HDS runs on unsupported W_2C, are established. The repeatability of both W_2C synthesis and catalytic activity with chemical stability are shown. The HDS of DBT was investigated using a fixed-bed reactor. The reaction was carried out at 613 K, under a 6 MPa total pressure of H_2. The global reaction follows two parallel routes. Under the experimental conditions, DBT has a single final product along each route, leading either to biphenyl through the direct desulfurization (DDS) pathway, or to cyclohexylbenzene through the hydrogenation (HYD) pathway. Accordingly, the HDS of DBT over W_2C presents a *true zero order* reaction to DBT along the DDS route, and a *true first order* reaction along the HYD route. The resulting global apparent first order rate with respect to DBT is linked to the selectivity towards these two routes. The kinetically true zero order rate along the DDS route corresponds to the saturation by DBT of all its active sites and, consequently, means that the HYD route is occurring on a second kind of sites. The presence of two kinds of sites is thus kinetically demonstrated and discussed in term of Coordinatively Unsaturated Sites (CUS).

1. Introduction and background

Due to increasing environmental constraints, and considering that N and S contents of crude oils depend on their origin leading to various S/N ratios, optimization of catalysts and catalytic hydrotreating processes still remain important targets for the final full removal of both sulfur- and nitrogen-containing compounds from fuels. Very low sulfur content in gasoil is beneficial for both the environment and longevity of engine catalytic converters, avoiding poisoning and subsequent deactivation of deNO_x and oxidation catalysts. The level of sulfur has been limited to less than 10 ppm [1,2].

It is generally recognized that hydrotreating catalysts need two main functions: hydrogenation and hydrogenolysis of C—S and C—N bonds.

Due to the formation of H_2S as a product of HDS, supported transition metal sulfides are commonly used as industrial hydrotreating catalysts able to be sulfur resistant and active for sulfur [3,4] and nitrogen (hydrodenitrogenation–HDN) [5–7] removals.

Transition metal nitrides and carbides, especially molybdenum and tungsten ones, present the two major functions considered above for hydrotreating (hydrogenation and hydrogenolysis of C—S and C—N bonds) and consequently have been found to be active materials for treating the so-called refractory S- and N-containing compounds, in hydrotreating processes [8–12]. The present work concerns the case of *unsupported* W_2C tungsten carbide.

* Corresponding author. Present address: SYNTHOS S.A. Chemików 1, 32-600 Oświęcim, Building E-182, Poland. Tel.: +48 602 503 809.
E-mail address: marco297@wp.eu (M. Lewandowski).
[1] On leave.

0926-3373/$ – see front matter © 2013 Elsevier B.V. All rights reserved.
http://dx.doi.org/10.1016/j.apcatb.2013.08.011

A temperature-programmed reaction method was introduced by Boudart and co-workers [13,14] for the synthesis of unsupported $Mo(W)_2N$ and $Mo(W)_2C$ powders with high specific surface areas. After synthesis, nitrides or carbides are pyrophoric, and a pulsed passivation step (gentle oxygen adsorption) is required to prevent a bulk oxidation of these materials on exposure to air. This can explain the detection of oxygen during EDS characterization and the presence of oxygen in elemental chemical analysis of materials, as also shown in the present work.

Dibenzothiophene (DBT) and alkyl derivatives are typical sulfur-containing compounds found in gasoils [15]; furthermore it is one of the model compound in HDS catalytic studies [8,16–20] and has thus been selected in the present work.

Considering the overall HDS equation of dibenzothiophene (DBT):

$$2DBT + 7H_2 = BPh + CHB + 2H_2S$$

H_2S is formed on the surface of the catalyst during the catalytic reaction, before desorbing. As a consequence, surface sulfide species are expected to remain *adsorbed* on the catalyst surface by the end of reaction runs. It is worthnoting that Xinping Duan et al. [21] also found that H_2S passivation was superior to conventional O_2 passivation in hydrotreating catalysis over nickel phosphide.

The HDS mechanism of DBT follows two main routes: the direct desulfurization (DDS) of DBT to biphenyl (BPh), and the hydrogenation (HYD) route to cyclohexylbenzene (CHB).

All elementary steps, in a catalytic cycle, turn over at the same rate, taking into account their stoichiometric number σ_ι [22,23]. Hydrotreating mechanisms may involve several hydrogenating elementary steps, before the C—S bond scission leading to HDS of the reactant. Therefore, as hydrogenation steps are involved in DDS and HYD catalytic cycles of HDS, the rate constants associated to these steps will regulate the turnover rate of the whole cycles. These rate constants depend on the hydrogenation function of the catalyst. Hydrogenation function is a key parameter for catalyst selection and metal carbides are very active for this function.

Molybdenum and tungsten carbides have been recognized to be very active in hydrogenation reactions; as an example, they are able to hydrogenate benzene at room temperature [24]. Furthermore, similar to precious metals, they are able to proceed to hydrogenolysis [25,26].

Mo and W carbides have also been shown to be very active in carbazole HDN in the conditions of hydrotreating [27,28].

During the last 15 years, several group active in this area have considered the formation of carbosulfide species [29–42].

(i) In the present work we first concentrated our effort on the understanding, at the molecular level, of the nature of the *true* tungsten catalyst working "during" HDS of DBT when starting with fresh unsupported W_2C. The surface structure and texture of the catalytic material have been investigated after HDS catalytic runs, as well as the surface chemical composition. We also studied the carbide stability after 5 days of HDS runs in the conditions of laboratory.

(ii) In a second part, the present work will detail the classical kinetics, at the molecular level, of the HDS of DBT over unsupported W_2C, in the full range of conversion (up to 100%), in well defined process conditions. Kinetic data will lead to a better understanding of the catalytic behaviour (activity, selectivity and composition of the active sites) of this unsupported carbide. « Classical kinetics » approach according to Boudart's concepts [23] will lead to a simulation of the kinetic behaviour of unsupported W_2C, using the kinetic laws based on the reaction pathways along the two routes of HDS of DBT.

2. Experimental

2.1. Materials

WO_3 (Fluka, ≥99.5%) was used as precursor of catalysts. The following gases were used: dihydrogen (H_2, Air Liquide, Custom grade C, purity > 99.995%), helium (He, Air Liquide, Custom grade C, purity > 99.995%), dioxygen (O_2, Air Liquide, Custom grade C, purity > 99.5%), and methane (CH_4, Air Liquide, Custom grade N30, purity > 99.9%). Dibenzothiophene, decaline, dimethyl disulfide (all supplied by Fluka, ≥98%) were used as reactants for the kinetic study.

2.2. Preparation of unsupported W_2C

Tungsten carbides were prepared using a modification of the standard procedure of Volpe and Boudart [14]. Tungsten trioxide (2 g) was introduced on a porous disc in a quartz reactor, and carburized with a flowing mixture of 10 vol% CH_4/H_2, with a flowing rate of 13.2 L g^{-1} h^{-1}. The temperature was increased linearly from 300 to 923 K at a rate of 45 K h^{-1} and held at this temperature for 1 h. Finally, sample was cooled to room temperature (RT) in the carburizing gas mixture. The sample was passivated prior to exposure to air. The process of passivation by chemisorption of oxygen, at room temperature and under atmospheric pressure, was carried out in situ in the same reactor than that used for the synthesis of catalysts. Well defined amounts of oxygen in helium were pulsed on the catalyst, up to the total amount necessary for obtaining an oxygen monolayer, avoiding any carbide oxidation. The temperature of reactor was carefully maintained at constant temperature.

2.3. Characterization of catalyst

The passivated catalysts were characterized before and after reaction by X-ray diffraction, specific surface area "S_g", and after reaction by HRTEM associated with EDS (lattice images, direct and reverse Fast Fourier Transforms, direct lattice fringes profiles, images of atomic steps, edges, corners) and elemental analysis of sulfur, carbon and tungsten was done only after HDS. Dynamic CO chemisorption for active site titration was carried out for fresh catalyst without passivation step.

Structural identification of W_2C tungsten carbide was determined by X-ray diffraction (XRD) using a SIEMENS D-5000 automatic diffractometer with the CuK_α monochromatized radiation. The identification of W_2C was done using the JCPDS file (No. 00-035-0776).

A Quantachrome–Quantasorb Jr was used for S_g measurements in dynamic conditions. The S_g of catalysts were obtained from the nitrogen adsorption/desorption plots at different partial pressures of nitrogen. Standard S_g measurement using the BET method was based on a three-point analysis consisting of mixtures of 10, 20 and 30 vol% N_2/He. The materials (100 mg) were degassed under flowing nitrogen at 623 K, for 2 h, before measurement.

CO chemisorption is a classical technique used for titrating metallic sites in Catalysis by Metals. Therefore, it is also widely used to titrate the noble metal-like active sites of transition metal carbides or nitrides, as suggested by Boudart and co-workers [14,24,43,44]. The CO uptake was performed "*in situ*" in the synthesis reactor, without passivating or exposing the fresh carbide to air. Pulses of a known quantity of CO (17 μmol) were injected, at regular intervals, on the sample at room temperature, in flowing He (40 cm^3 min^{-1}) purified by an oxygen trap (Oxysorb, Messer Griesheim). After each injection, the amount of CO which has not been adsorbed was measured using a conventional device equipped with a TCD. The injections were continued until CO saturation of the

surface. Data were processed and the number of micromoles of CO chemisorbed per gram of sample was determined.

Elemental analysis of the solids was performed by the "Service Central d'Analyse du Centre National de la Recherche Scientifique (Vernaison, France)". Amounts of hydrogen and carbon were determined by combustion of the solid and analysis of the effluent gases in "microanalyser C.H.N". Tungsten analysis was realized by the ICP method: atomic emission spectroscopic principle. An amount of sulfur was determined by LECO SC 144 instruments with standard IR detection of sulfur. After HDS reaction runs catalysts were kept in the reactor (H_2 atmosphere) for cooling to room temperature. They were quickly removed from the reactor and kept in *n*-heptane for storage before analysis. According to Xinping Duan et al. [21] catalyst may be passivated by H_2S produced by the reaction. Amounts of residual carbon and sulfur (as surface adsorbed sulfur species), were determined by combustion of the solid and analysis of the effluent gases. Tungsten analysis was realized by plasma emission spectroscopy.

The HRTEM study was performed using a JEOL JEM 2010 UHR equipped with a LaB_6 filament and operating at 200 kV. The images were collected with a 4008 × 2672 pixels CCD camera (Gatan Orius SC1000) coupled with the DIGITAL MICROGRAPH software. The chemical analysis was obtained by a selected energy-dispersive X-ray spectroscopy (EDS) microanalyser (PGT- IMIX PC) mounted on the microscope. The sample was crushed and dispersed in ethanol. A drop of this solution was deposited on a lacey carbon film-copper grid for the HRTEM observations.

2.4. Kinetic study of HDS of DBT

The HDS of DBT was conducted with a down flow fixed-bed reactor in a high-pressure flow system. All catalytic runs were performed over 0.6 g of catalyst for HDS reaction. The liquid feed, consisting of 1.5 wt% solution of DBT in decaline, was delivered to the flow manifold by a high pressure piston pump (Gilson model 307). Hydrogen flow and total pressure were controlled by a mass flow controller Brooks 5850TR and a back pressure regulator Brooks 5866, respectively. Temperature of the oven was regulated using a temperature controller Hamyoung MX9.

The kinetic study of the HDS process was carried out at a total pressure of 6 MPa, at 613 K, with a H_2/feed volume ratio of 600 and for contact times (t_c) between 0.07 and 0.8 s. The contact time (t_c) was defined as follows: t_c (s) = catalyst volume (cm^3)/(H_2 flow + feed flow) ($cm^3\ s^{-1}$). The catalyst volume was 0.4 cm^3 and the total flowrate of liquid feed was in the range from 0.05 to 0.6 $cm^3\ min^{-1}$.

The liquid products of the reaction were collected every hour and analyzed by gas chromatography (HP 4890) using a capillary column (HP1, 30 m × 0.25 mm × 0.25 μm) and a FID detector. Before reaction, the carbide catalysts were pre-treated "*in situ*" for 10 h, by flowing a mixture of 70 ppm dimethyldisulfur (DMDS)/decaline in hydrogen carrier gas (60 $cm^3\ min^{-1}$), at the temperature of reaction and at a total pressure of 6 MPa. This pre-treatment corresponds to the pre-stabilization of the catalyst surface working in the HDS conditions during H_2S production.

3. Results and discussion

3.1. Sulfur species adsorbed after runs over unsupported W_2C stabilized during HDS of DBT. Nature of active sites

Two main results are presented below: before (fresh W_2C) and after hydrodesulfurization of DBT. Two kinds of analyses are conducted: at global and molecular/atomic levels.

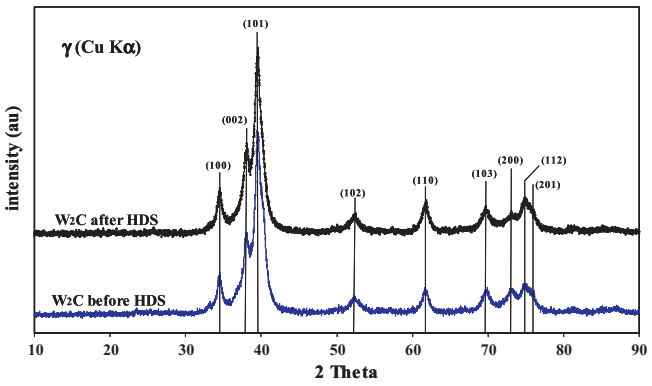

Fig. 1. XRD patterns of W_2C before and after HDS reaction of DBT.

Table 1
Elemental analysis data for W_2C after HDS: comparison with theoretical (W and C) wt%.

	Theoretical			Analysed			Corrected for passivation	
	wt. %							
	C	W	S	C	W	S	C	W
W_2C after HDS	3.2	96.8	-	2.9	88.3	1.2	3.2	96.8
Total	100			92.4			100	
C+W				91.2				
WS_2		74.2	25.8					
$S\%_{W2C}/S\%_{WS2}$	**0.05**							

The XRD pattern of the fresh synthesized tungsten carbide is shown on Fig. 1. It exhibits all reflections lines of the hexagonal compact β-W_2C structure (JCPDF File N° 01-035-0776).

The specific surface area (S_g) of the fresh passivated W_2C synthesized at 923 K was 13 $m^2\ g^{-1}$.

According to Sajkowski and Oyama (over Mo carbide and nitride) [44] and Boudart and co-workers (over Mo_2C) [45] the active "W" surface sites of unsupported W_2C can be titrated by CO. If W_2C *does not suffer any bulk sulfurization during* HDS, the density of surface "W" sites titrated by CO before HDS reaction gives the opportunity for a quantitative analysis of the stabilized surface state of the carbide working in HDS conditions. In this work, CO uptake titration over non-passivated unsupported W_2C, led to 70 μmoles of chemisorbed CO per gram of sample. Assuming with Boudart and co-workers that one CO molecule titrates only one noble metal-like tungsten atom [24,44,45], and considering that the theoretical average density of surface tungsten atoms of unsupported W_2C is 1.10^{19} W atoms m^{-2}, it can be calculated that 28% of the surface tungsten atoms of the W_2C sample have a precious metal-like behaviour. CO is titrating all clean terraces and edge + corner sites. The kinetics of the HDS of DBT will lead to the conclusion that two kinds of sites are necessary for this reaction.

The XRD pattern of W_2C after HDS of DBT is also reported in Fig. 1. It is clear that the bulk structure of tungsten carbide did not change, remaining as the β-W_2C phase. This was simarly observed by Aegerter et al. [30] for Mo_2C.

After catalytic run the specific surface area of W_2C did not changed, and was 15 $m^2\ g^{-1}$. Table 1 shows the results of elemental analysis of a passivated unsupported W_2C sample after hydrodesulfurization of DBT, together with the theoretical weight percent of W, C and S calculated for WS_2 and W_2C. The second line from down of Table 1 is for sake of comparison with unsupported WS_2. As it can be seen, elemental analysis does not match the 100% of

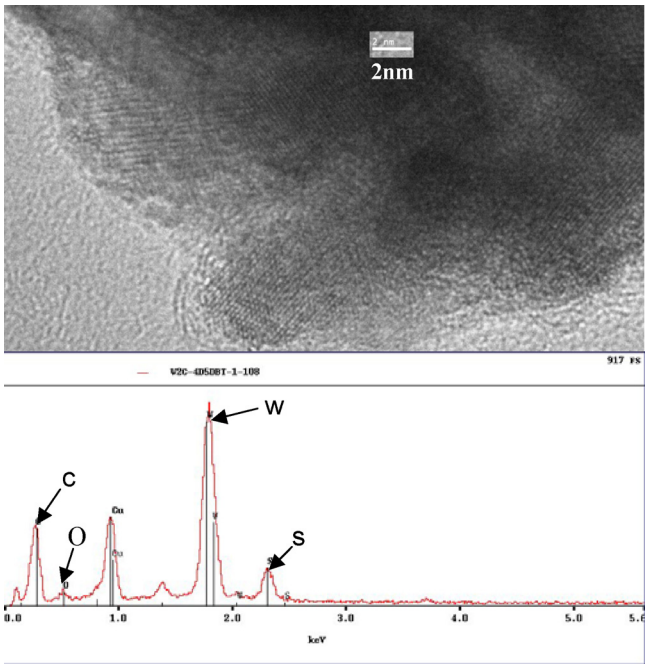

Fig. 2. HRTEM image of a W_2C domain after 5-day HDS reaction, together with the corresponding EDS analysis.

[W + C + S]wt%, this material balance being equal to 92.4 wt%: the difference is due to oxygen uptake during the necessary exposure to air before analysis, see Fig. 2.

Various materials based on W and C balance can be compared. Considering the experimental values of Wwt% and Cwt% for W_2C sample (Table 1), the sum [W% + C%] is [88.3 + 2.9] = 91.2 wt%.

The experimental value of W% in the "fresh W_2C sample" is therefore: 88.3/91.2 = 96.8%, which is exactly the theoretical value, as shown Table 1.

The elemental analysis also leads to the experimental Cwt% value: 2.97/91.25 = 3.2 wt%, corresponding to the theoretical value (3.2 wt%) reported Table 1.

Finally, the ratio of the experimental S% value in the W_2C sample after HDS reaction, to the theoretical S % of bulk WS_2: $S\%_{W_2C}/S\%_{WS_2} = 1.2/25.8$, is about 0.05. *It means that the W_2C sample is really far from a deep sulfurization after 5 days of HDS run*.

Comparing the above 0.05 ratio between S contained in the W_2C sample to that in WS_2 bulk material, (25.8 wt%, Table 1), considering the detection of W_2C and the absence of detection of WS_2 by XRD (Fig. 1) after HDS, and taking into account that H_2S is a product of the catalytic HDS process, i.e. produced on the unsupported W_2C surface, every sulfur species of elemental analysis (Table 1) can be considered to remain adsorbed on the W_2C carbide surface after HDS reaction. This is quite consistent with next section results, when comparing the number of S-surface species to the theoretical crystallographic total number of surface tungsten atoms.

Table 1 shows that the W_2C sample have 1.2 wt% S per g; for 13 $m^2\ g^{-1}$, it corresponds to 1.78×10^{19} S atoms m^{-2}. Considering 10^{19} theoretical crystallographic total surface W atoms m^{-2}, and 1.78×10^{19} S surface atoms m^{-2}, it means that there are close to 2 S for 1 W, if all S atoms are only adsorbed on the W_2C surface, without any diffusion in sublayer of W_2C, as it will be shown by HRTEM hereafter, at the atomic level.

Partial conclusion on the global characterization of unsupported W_2C can already be given. XRD patterns of W_2C and the above data from elemental analysis show the presence of a very small content of sulfur, consistent with a quantitative formation of a "monolayer" of "surface" S–W–S species due to "S ad-species", as calculated above. Among these S–W–S species, only 30% are active in HDS reaction because they should correspond to two special coordinatively unsaturated sites (CUS) of W_2C platelets, as it will be demonstrated in the next section at the atomic level, by HRTEM associated to EDS, and later by kinetics.

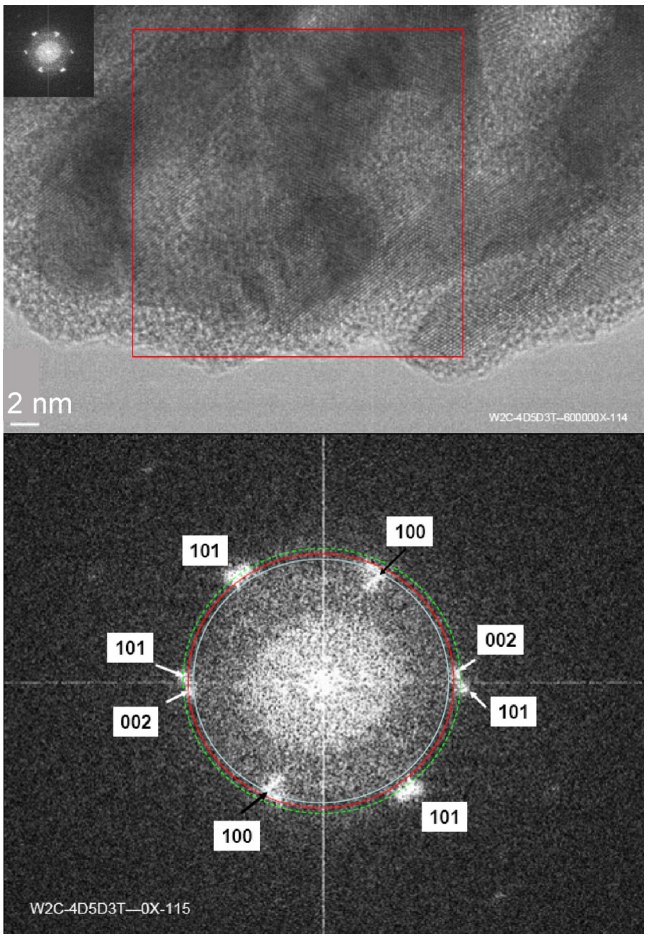

Fig. 3. Fast Fourier Transform (FFT) (lower image) on a W_2C grain domain (selected frame in the HRTEM image).

Noteworthy is that the monolayer of adsorbed S species on surface tungsten atoms determined after runs, should suffer in the experimental conditions of HDS reaction (60 bar hydrogen at 613 K) a so-called "*reactive-desorption*" as H_2S, leading to a cleaning of tungsten carbide active sites, and allowing the HDS reaction to proceed.

To describe the nature of active sites in HDS reaction, a detailed characterization of the texture and structure of W_2C at the atomic level can be considered. The HRTEM image of several crystallites of W_2C after HDS of DBT together with the EDS analysis of the grain are shown Fig. 2. EDS analysis is a bulk technique made on the whole domain of the grain shown on Fig. 2. A weak sulfur peak is detected. The weak oxygen peak comes from the passivation of the sample during exposure to air after HDS reaction. This oxygen can also be due to the oxidation of adsorbed sulfur species remaining on the carbide surface after HDS reaction. The peak intensity ratio S/W is quite low, compared to the expected ratio for bulk WS_2 (1/1) on this equipment, and in accordance with the results from XRD and elemental analysis of the catalyst after HDS. This leads to the first conclusion that there is no bulk sulfurisation of W_2C.

The texture of W_2C shows the overlapping of platelets (Fig. 3). A new domain has been selected on the same sample of W_2C after

5-day HDS run. Several directions of the same lattice fringes show that the grain is not a single crystal, as shown hereafter.

Crystallographic planes of W_2C observed by both lattice fringes and lattice structure in HRTEM image (Fig. 3) were determined applying Fast Fourier transform (FFT) on the W_2C grain domain selected in the frame of this upper HRTEM image. As it is well known, the Fourier transform yields a diffraction pattern similar to the original electron diffraction pattern, allowing similar indices to be assigned to the spots of FFT pattern. The indices of FFT spots were assigned (Table 2) according to the XRD JCPDS file (No. 01-035-0776).

Contributions of (1 0 0), (0 0 2), (1 0 1) crystallographic planes to the HRTEM image of W_2C were also determined by applying a Reverse Fast Fourier Transform (Fig. 4a–d) using the different couples of diffracted spots of FFT pattern of Fig. 3: it permits to convert from the Fourier space back to the real space. These images permit to partially represent the real crystallographic lattice of W_2C (Fig 4a–d). Reverse FFT image Fig. 4a has been performed using a mask selecting the couple of diffracted spots (1 0 0). It shows that the corresponding planes of the HRTEM image are covering the whole selected grain domain. The orientation of the lattice fringes on the

Table 2
($h\,k\,l$) indices assigned to FFT spots and experimental and JCPDS $d_{(h\,k\,l)}$ values.

($h\,k\,l$)	$d_{(h\,k\,l),\,exp}$ (Å)	$d_{(h\,k\,l),\,JCPDS}$ (Å)
(1 0 0)	2.55	2.59
(0 0 2)	2.34	2.36
(1 0 1)	2.26	2.27

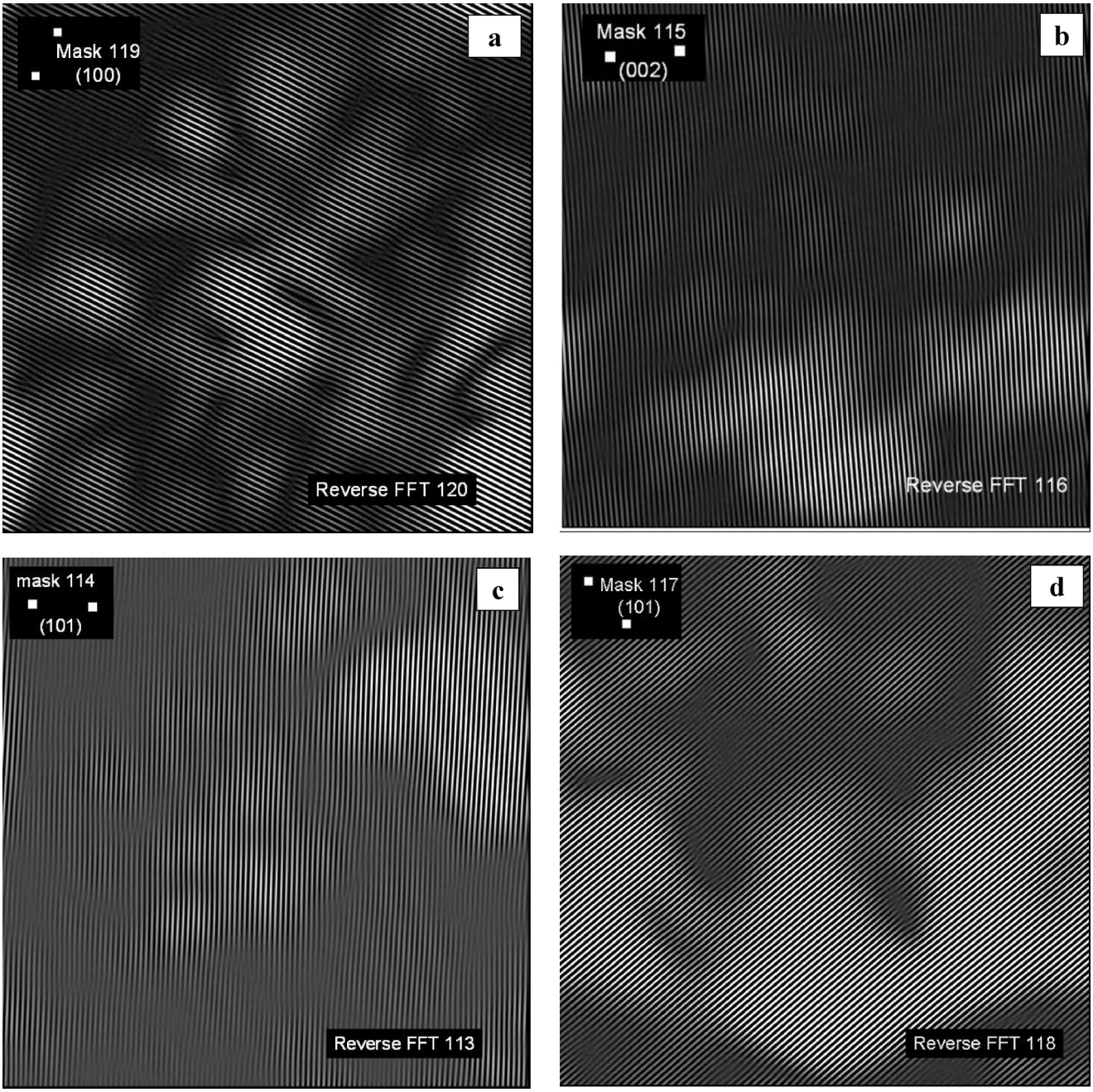

Fig. 4. (a–d) Reverse Fast Fourier Transform using diffraction spots of the FFT pattern in Fig. 3. The following W_2C lattice fringes are identified: (a) (1 0 0); (b) (2 0 0); (c) (1 0 1); (d) (1 0 1). For sake of simplification the ($h\,k\,l$)s of hexagonal system have been reported as ($h\,k\,l$).

reverse FFT image are perpendicular to the direction of the two spots as expected by the theory.

The same comment applies to the reverse FFT image of the grain, using the two (0 0 2) spots (Fig. 4b). The two Fig. 4c and d demonstrate that there are two overlapping platelets corresponding to the (1 0 1) spots.

As a partial conclusion of this FFT and reverse FFT studies, it can be concluded that after HDS reaction (5-days of run) W_2C appears to be quite well stable, without any bulk sulfurization. Furthermore, the texture of W_2C corresponds to platelets whose upper planes are perpendicular to electron beam and parallel to both the microscope grid and image.

To confirm with high precision the interlattice distances, direct lattice fringes measurement using a profile programme (Fig. 5) has been used on another domain of the same sample of W_2C after 5 days of HDS run. The value of the interlattice plane distance corresponds to $d_{(1\,0\,0)}$ (0.25 nm) identifying again a W_2C platelet grain.

Fig. 6 presents the HRTEM of a domain of W_2C after HDS, where $d_{(1\,0\,1)}$ and $d_{(1\,0\,0)}$ of W_2C have been identified. The corresponding (1 0 1) and (1 0 0) lattice planes are perpendicular to the picture and parallel to the electron beam, evidencing the platelet texture of W_2C. Once again W_2C is identified, in agreement with XRD. Fig. 6b is the negative image of Fig. 6a, giving a contrasted image of the platelet texture with the formation of steps of W_2C after reaction. Fig. 6b also clearly shows the presence of terraces, steps, kinks and ledges of W_2C platelets.

The edges of the W_2C grain are quite clean – without polymeric carbon deposit. This is in concordance with elemental analysis, the C content being near the value for pure W_2C.

The textural organization of the different orientations of lattice planes explains the formation of the simplified like-Debye-Scherrer FFT pattern interpreted on Fig. 3.

Active sites are W atoms as seen on Fig. 6 (HRTEM) where terraces, edges and corners are well defined. Fig. 6 gives an ideal image of the so-called Coordinatively Unsaturated Sites (CUS) of W_2C platelets, the number of dangling bonds defining the degree of unsaturation of active sites.

Considering that DDS route only needs the formation of dihydroDBT before C—S bond hydrogenolysis, and HYD route needs 3 successive hydrogenation steps before C—S bond hydrogenolysis", the role of CUS tungsten sites in HDS reaction can be discussed as follows.

Terrace-W atoms only have 1 dangling bond. Two adjacent sites on terrace are able to dissociate dihydrogen similarly to precious metals process, in the conditions of HDS reaction (60 bar H_2).

The edge-W atoms have 2 dangling bonds permitting either H_2 dissociation, or adsorption-reaction of the S-containing molecule such as DBT. Due to their proximity of terraces, they are able to proceed to DBT hydrogenation owing to H atom spillover from terraces to edges, producing the dihydroDBT.

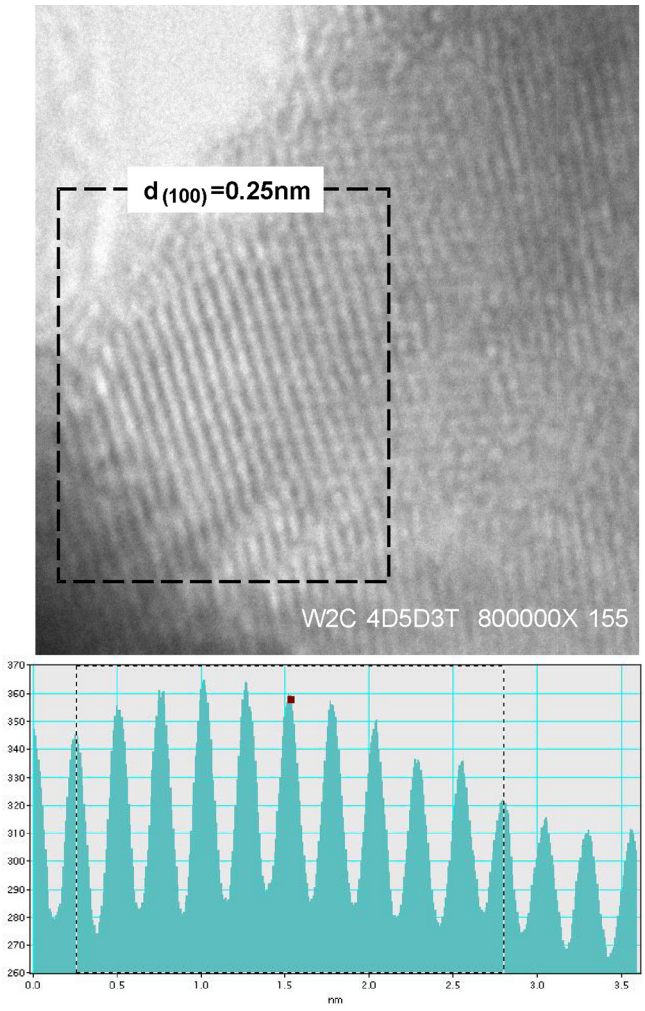

Fig. 5. Direct lattice fringes measurement using a profile programme. Identification of $d_{(1\,0\,0)}$ of W_2C.

W-corners atoms present 3 dangling bonds permitting both reactant and hydrogen adsorption. They can theoretically proceed to the HYD route.

According to literature [46–48] it can be assumed that active sites are edge and corners sites of W_2C platelets in HDS reaction. This assumption will have to be confirmed in the future by varying the grain morphology and therefore the ratio of the various active sites.

According to Nigra about "Molecular-Level Structure-Function Relations in Gold Nanoparticle Catalysis", [46] coordinatively unsaturated corner and edge atoms have been hypothesized to

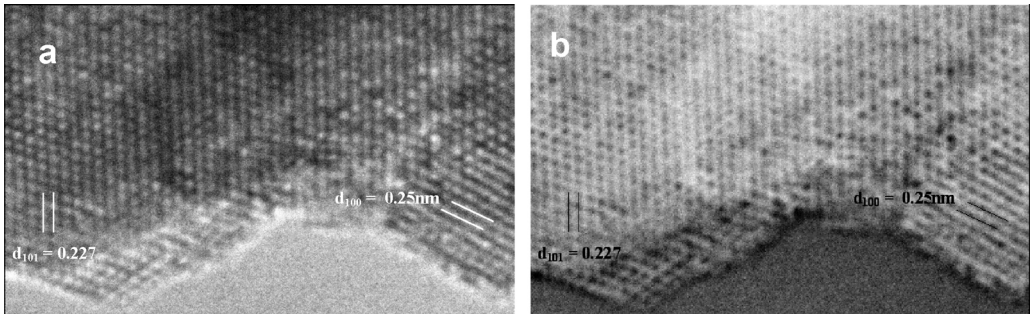

Fig. 6. HRTEM of a domain of W_2C after HDS, where $d_{(1\,0\,1)}$ and $d_{(1\,0\,0)}$ of W_2C have been identified. For sake of better representation of steps, (b) is the negative image of (a).

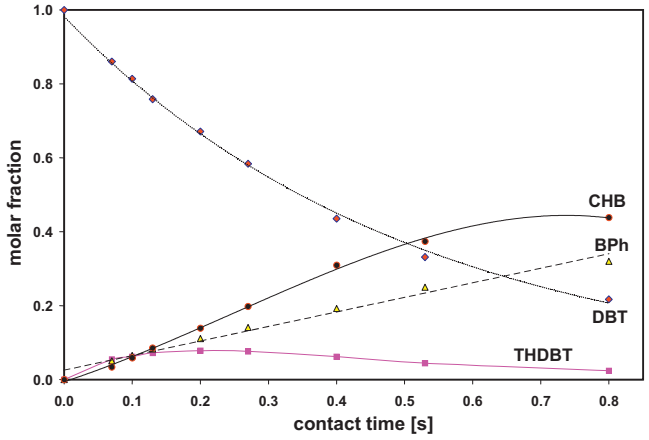

Fig. 7. Mathematical fitting (lines) of experimental data (points) using exponential or polynomial functions. (♦) dibenzothiophene (DBT), (■) tetrahydrodibenzothiophene (THDBT), (▲) biphenyl (BPh), (●) cyclohexylbenzene (CHB).

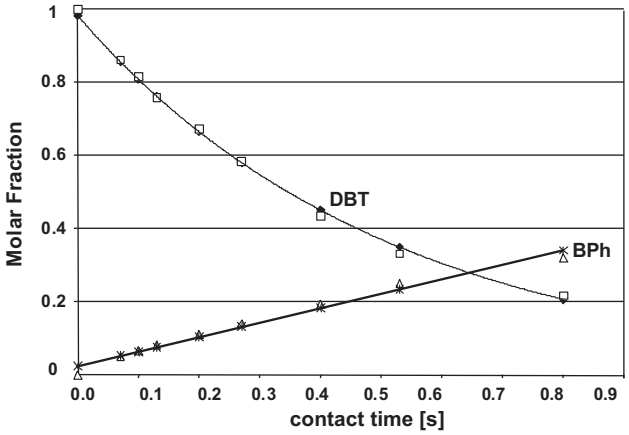

Fig. 8. Experimental and simulated plots for DBT and BPh over bulk W_2C. Experimental values are those reported on Fig. 7. (□) DBT experimental, (♦) DBT simulated = 0.98 exp(−1.946 *t*) with R^2 = 0.99, (Δ) BPh experimental, (Ж) BPh simulated = 0.39 *t* + 0.025 with R^2 = 0.98.

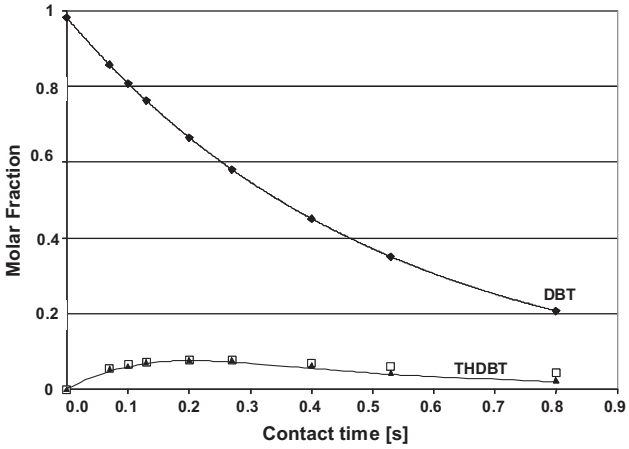

Fig. 9. Fitting between experimental and simulated THDBT plots over bulk W_2C. The DBT trace is given as a scale reference. (♦) DBT simulated = 0.98exp(−1.946t) with R^2 = 0.99, (▲) THDBT experimental, (□) THDBT simulated.

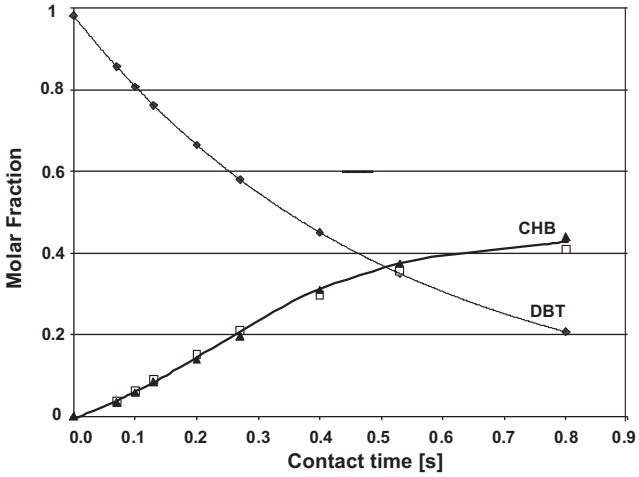

Fig. 10. Fitting between experimental and simulated CHB plots over bulk W_2C. The DBT trace is given as a scale reference. Note that CHB initial slope indicates that CHB is a secondary product. (♦) DBT simulated = 0.98 exp(−1.946 *t*) with R^2 = 0.99, (▲) CHB experimental, (□) CHB simulated.

have the highest activity of sites responsible for many catalytic reactions on a metal surface. It is demonstrated that the most coordinatively unsaturated sites (the corner atoms) are the most active atoms by over an order of magnitude as compared to uncoordinated edge atom sites, whereas terrace sites with only one dangling bond are completely inactive.

Kogan et al. [47] have also proposed 2 kinds of sites, and the coordinatively unsaturated sites that directly participate in the reaction, for HDS of thiophene molecules.

Wang and Iglesia [48] considered, in the case of small Pt clusters, "the prevalence of coordinatively unsaturated corner and edge sites in the HDS of thiophene". According to Wang and Iglesia [49] "one site is proposed to catalyze direct C—S cleavage through the involvement of sulphur vacancies (coordinatively unsaturated sites, CUS) at edges of lamellar MoS_2 structures. The other site catalyze hydrogenation and hydrogenolysis of C—C and C—S bonds and resides near the edges of MoS_2 terraces".

In the kinetic section, it will be shown that two different active sites are necessary for the two routes of HDS pathways to occur.

All HRTEM images, such as in Fig. 6, are characteristic of typical representation of single crystal surface.

As a conclusion, all these structural and textural results are consistent with:

a) The presence of W_2C after 5 days of HDS runs.
b) The presence of a small content of sulfur consistent with the quantitative formation of surface "S ad-species".
c) The presence of terraces, steps, kinks, corners, edges and ledges of W_2C.

The results of the classical molecular kinetics simulation hereafter will unambiguously indicate the necessity for two types of active centres on the W_2C tungsten carbide surface involved in HDS process.

3.2. *Kinetics of HDS of DBT over W_2C*

Fig. 7 shows the experimental plots of all products: tetrahydrodibenzothiophene (THDBT), biphenyl (BPh), cyclohexylbenzene (CHB) and DBT.

The first stage of the study is therefore to use true macrokinetics equations to fit experimental data. Simulation of the experimental plots of this reaction, based on true first and zero order reactions, will provide global rate constants and kinetic laws (Figs. 8–10 and 12).

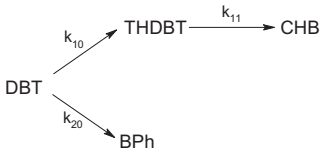

Scheme 1. Simplified pathway for the two parallel reaction routes (HYD above, DDS below) during the HDS of DBT over bulk W_2C.

In a second stage, macro-kinetics laws will then be detailed at the molecular level, using elementary step network and the quasi-stationary state approximation (QSSA) [22,23]. Concerning the macro-kinetics behaviour of HDS of DBT over W_2C, Fig. 7 reports the molar fractions of the detected products and the reactant at different contact times (t_c). The two routes indicated in Scheme 1 correspond respectively to the appearance of biphenyl for the "direct desulfurization" (DDS) one, and to tetrahydrodibenzothiophene and cyclohexylbenzene, for the "hydrogenation" (HYD) one. Following these observations, macro-kinetics mechanism of HDS of DBT can be simplified as shown in Scheme 1, where BPh is not hydrogenated to CHB.

Let us note that it is now well-established that carbides are very active in hydrogenation of unsaturated hydrocarbons, and BPh alone can be hydrogenated at H_2 pressure and temperature of HDS. Nevertheless, the addition of 4,6-DMDBT in the feed during the hydrogenation reaction, leads to a strong inhibition of BPh hydrogenation as described by P. Da Costa et al. [50]. Furthermore, in HDS conditions, 4,6-DMDBT is so strongly adsorbed on carbides that it is strongly competing over Mo_2C with the just-produced BPh provoking its desorption and avoiding its hydrogenation to CHB.

The same conclusion have been found for HDS of DBT over Mo_2C and bulk W_2C by Szymańska-Kolasa et al. [51].

Fig. 8 shows that the decrease of the DBT molar fraction follows an exponential decrease implying a global (apparent) first order rate law with respect to DBT [22,23]. Based on this assumption, the molar fractions of DBT were recalculated versus contact time and Eq. (1) was determined:

$$[\mathrm{DBT}]_{\mathrm{calc.}} = 0.98\ \exp(-1.95 \times t) \quad (1)$$

The 0.98 value corresponds to the initial DBT mole fraction, experimentally equal to1 and the macro-kinetics global constant is equal to $k_{\mathrm{global,\ DBT}} = 1.95\ \mathrm{s}^{-1}$.

According to Scheme 1, the consumption of DBT follows the classical macro-kinetics of twin reactions [22,23] and the global rate of consumption of DBT should be written as follows:

$$r_{\mathrm{DBT\,cons.}} = r_{\mathrm{DDS}} + r_{\mathrm{HYD.}} \quad (2)$$

with

r_{DDS}: global rate conversion of DBT along the DDS route.

r_{HYD}: global rate conversion of DBT along the HYD route.

From Fig. 8, as the formation rate of BPh (unique product of the DDS route) is constant, it can be assumed that the consumption rate of DBT along the DDS route should also be linear and can be kinetically described by a zero order r_{DDS}. This true behaviour means that the active sites working along the DDS route are constantly saturated in the range of our operating conditions. This conclusion is quite consistent with the very strong adsorption of DBT avoiding the hydrogenation of BPh to CHB (Scheme 1 and [51]). The molar fraction of BPh versus contact time can be described by the following Eq. (3):

$$[\mathrm{BPh}] = 0.39 \times t + 0.025 \quad (3)$$

According to Scheme 1, k_{20} is the global rate constant of the DDS route and corresponds graphically to the director coefficient of Eq. (3), i.e., it is equal to $0.39\ \mathrm{mol\,s}^{-1}$.

Table 3
Selectivity of bulk W_2C and bulk Mo_2C (for sake of comparison) in HDS of DBT Temperature of reaction = 613 K, H_2 pressure = 60 bars, H_2/feed = 600.

t_c [s]	Selectivity [BPh/CHB]		
	Mo_2C	W_2C	SMo_2C/SW_2C
0.80	2.31	0.73	3.2
0.53	1.91	0.67	2.9
0.27	1.97	0.71	2.8
0.13	2.67	0.97	2.7
0.10	3.07	1.17	2.6

In contrast, the HYD route presents all the macro-kinetics features of successive first order reactions. Indeed, the molar fraction of THDBT intermediate goes through a maximum as for an intermediate of successive 1st order reactions (Fig. 9). It can be considered as a primary product according to its initial slope, whereas the CHB corresponds to the final product.

Taking into account, the material balance, and the macro-kinetics equations for successive first order reactions [22,23], the rate constants k_{10} and k_{11} (Scheme 1) were calculated: $k_{10} = 1.18\ \mathrm{s}^{-1}$ and $k_{11} = 11.7\ \mathrm{s}^{-1}$.

From these set of rate constants, all mole fractions were calculated.

$$[\mathrm{THDBT}] = \left[\frac{1 \times 1.18}{11.7 - 1.18}\right] [\exp(-1.18 \times t) - \exp(-11.7 \times t)] \quad (4)$$

and

$$[\mathrm{CHB}] = 1 - ([\mathrm{DBT}] + [\mathrm{BPh}] + [\mathrm{THDBT}]) \quad (5)$$

The following plots (Figs. 9 and 10) show the good agreement between experiment, theory, and complete macro-kinetics simulation respectively for [THDBT] and [CHB]. It must be emphasized that the global first order consumption rate of DBT corresponds in fact to the sum of a zero order rate (along the DDS route) and a first order rate (along the HYD route) routes. Therefore, the total consumption rate of DBT is an apparent first order rate.

The very striking result is that if the DDS catalytic cycle occurs according to a zero order and corresponds to the saturation of a first kind of sites of W_2C working along the DDS route, it means that the elementary steps along the HYD route have to take place on a different kind of sites, which are not saturated by the reactant (leading to a first order process). As a consequence, it can be considered that W_2C presents two kinds of active sites: one for the DDS route (saturated), one for the HYD route, (unsaturated).

Hynaux et al. [52,53] observed a similar behaviour over a molybdenum carbide supported over a carbon material. Based on DFT study, Tominaga and Nagai [54] also postulated that HDN of carbazole took place on two active sites over Mo_2N, similar to W_2C.

Table 3 presents the selectivity between the DDS and the HYD routes over W_2C, calculated as the molar ratio of [BPh]/[CHB] and compare to selectivity over Mo_2C. It can be concluded that the HYD route leading to CHB during HDS of DBT is a dominant route over W_2C contrary to the case of Mo_2C.

From the above macro-kinetics study of HDS of DBT, two different global orders were determined along hydrogenation and direct desulfurization routes. Scheme 2 presents the two catalytic cycles kinetically uncoupled (no common intermediate, two different active sites of W_2C platelets). Scheme 2a corresponds to the DDS route leading to BPh. According to the QSSA theory [22,23], the rate of the DDS cycle is given by the first elementary step and is described by the following Eq. (6):

$$r\mathrm{BPh} = k'_{20}[*\mathrm{DBT}] \quad (6)$$

As all sites are saturated:

$$r\mathrm{BPh} = k'_{20}[\mathrm{L}_1] = \mathrm{const} = k_{20} \quad (7)$$

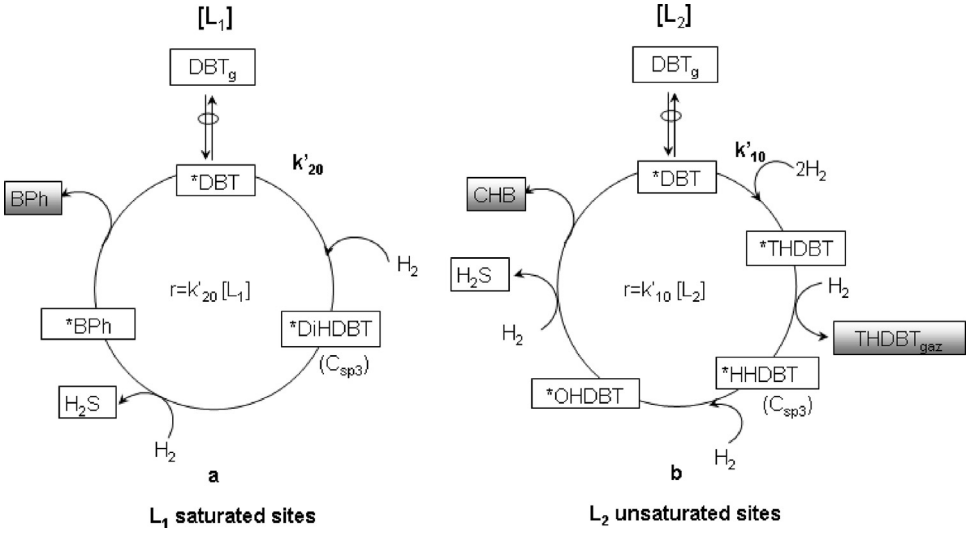

Scheme 2. Catalytic cycles of HDS of DBT over bulk W_2C. (a) DDS route, over L_1 sites (b) HYD route over L_2 sites.

k_{20} being the initial macro-kinetics rate constant. To conclude, a zero order rate with respect to DBT can also be determined at a molecular scale along the DDS route. If L_1 sites are saturated, we need the L_2 second kind of active sites for the hydrogenation route.

Scheme 2b, corresponds to the HYD route leading to CHB. As previously discussed, the rate of the HYD route is a first order rate with respect to DBT i.e. the L_2 sites are not saturated. According to the QSSA theory [22,23], the molecular rate of the HYD cycle follows Eq. (8):

$$r_{HYD} = k'_{10}[*DBT] \tag{8}$$

Considering the adsorption equilibrium of DBT over L_2 sites the equilibrium constant can be written as follows in Eq. (9):

$$K_{DBT} = \frac{[*DBT]}{[DBTg]\,[*]} \tag{9}$$

with [*] being the free L_2 sites concentration, the balance on L_2 active sites being:

$$[L_2] \sim [*] + [*DBT] \tag{10}$$

[*DBT] being taken as the most abundant adsorbed intermediate [22]

$$[*DBT] = \frac{[L_2]K_{DBT}[DBT]}{1 + K_{DBT}[DBT]} \tag{11}$$

$$r_{HYD} = k'_{10}[*DBT] = \frac{k'_{10}[L_2]K_{DBT}[DBT]}{1 + K_{DBT}[DBT]} \tag{12}$$

In order to get a rate law similar to a first order rate with respect to DBT, it has to be considered that [*] » [*DBT] and, as a consequence, $K_{DBT}[DBT] \ll 1$. Therefore, Eq. (12) can be simplified to the following Eq. (13):

$$r_{HYD} = k'_{10}[L_2]K_{DBT}[DBT]^1 = k_{10}[DBT]^1 \tag{13}$$

k_{10} being the initial macro-kinetics rate constant and the rate law being first order with respect to DBT, which means that DBT is weakly adsorbed over L_2 sites.

During the catalytic run no deactivation of catalyst was observed in the applied conditions, as shown on Fig. 11 (conversion of DBT vs. time on stream). To confirm the catalystic activity and selectivity of tungsten carbide, a second synthesis of catalyst has been

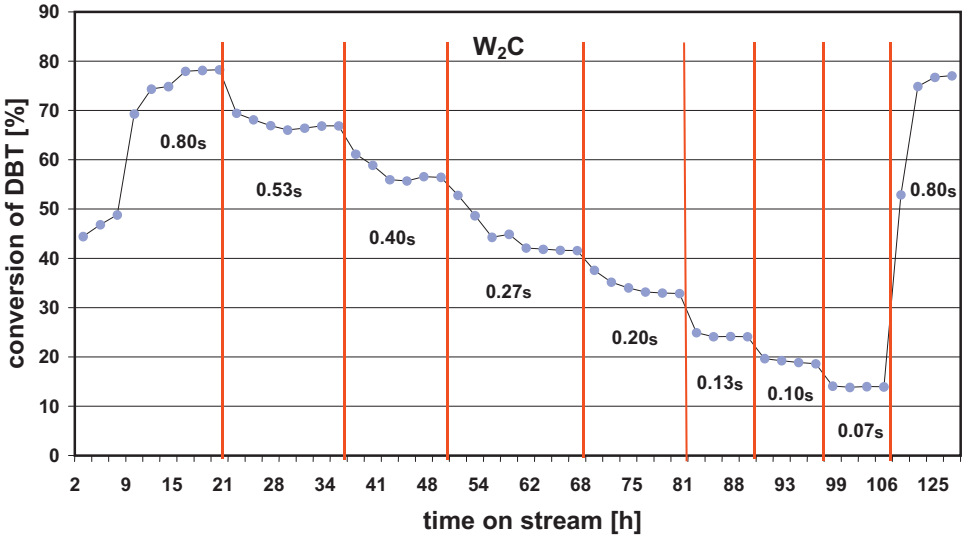

Fig. 11. Conversion of DBT versus time on stream, over bulk W_2C. Experimental run for testing catalyst stability by varying residence time (in second as shown on the graph) and coming back to the initial residence time after 125 h.

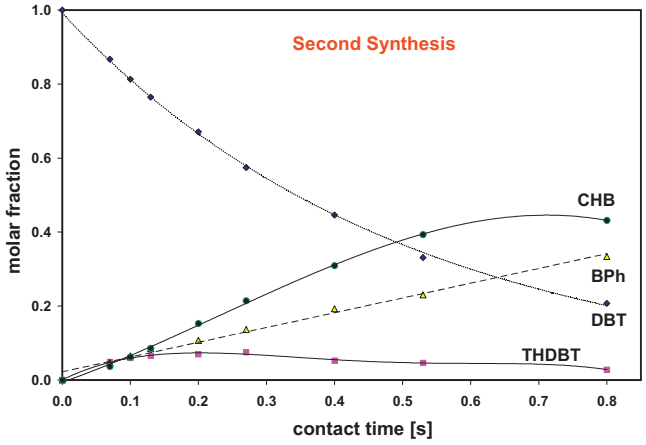

Fig. 12. Experimental plots for DBT = 0.99 exp(−1.994 t) R^2 = 0.998, BPh = 0.40 t + 0.022 with R^2 = 0.989, THDBT and CHB over bulk W_2C from second synthesis of W_2C.

done and the same catalytic test was carried out. The results given on Fig. 12 show the value of the apparent rate constant $k_{global,\ DBT} = 1.994\ s^{-1}$, close to the previous value: $1.946\ s^{-1}$. Furthermore, $k_{20} = 0.39$ mol s^{-1} is very similar to 0.40 mol s^{-1} obtained for first and second test, respectively.

4. Conclusions

- Catalyst characterization and more particularly XRD patterns, elemental analysis, HRTEM and FFT and reverse FFT studies, have shown that after long duration HDS reaction (5 days), W_2C appears to be quite stable, without any bulk sulfurization.
- The texture of W_2C corresponds to platelets permitting to consider coordinatively unsaturated sites as active in HDS.
  All structural and textural results are consistent with:
  a) The presence of W_2C after 5-days of HDS run
  b) The presence of a small content of sulfur consistent with the quantitative formation of "S ad-species" after reaction.
  c) The presence of terraces, steps, kinks, corners, edges and ledges of W_2C.
  d) The results of the classical molecular kinetics simulation unambiguously indicate the necessity for two types of active centres on the tungsten carbide surface involved in HDS.
- The global experimental rate of the hydrodesulfurization of DBT is a first order rate with respect to the reactant over bulk W_2C; it has to be underlined that it is only an "apparent" first order rate. Indeed, it corresponds to the sum of a zero order rate (along the DDS route) and a first order rate (along the HYD routes) with respect to DBT.
- The crucial point is the presence of two kinds of actives sites over bulk tungsten carbides; according to literature [46,48] it can be assumed that active sites are edge and corners sites of W_2C platelets HDS reaction. This assumption has to be confirmed in the future by varying the grain morphology and therefore the ratio of active sites.
- Using all determined macro-kinetic constants, a classical kinetic fitting of all molar fractions of reaction species versus contact time was observed, for the HDS of DBT over bulk W_2C.

Acknowledgements

CNRS, Polish Academy of Science and French Foreign Office are greatly acknowledged for their financial support in the framework of Jumelage "Carbonaceous and catalytic materials for environment".

References

[1] J.A.R. van Veen, S.T. Sie, Fuel Process. Technol. 61 (1999) 1.
[2] F. Hernández-Beltán, R. Quintana-Solórzano, J. Sáchez-Valente, F. Pedraza-Archila, F. Figueras, Appl. Catal. B: Environ. 42 (2003) 145.
[3] K. Sakanishi, T. Nagamatsu, I. Mochida, D.D. Whitehurst, J. Mol. Catal. A: Chem. 155 (2000) 101.
[4] D. Zuo, D. Li, H. Nie, Y. Shi, M. Lacroix, M. Vrinat, J. Mol. Catal. A: Chem. 211 (2004) 179.
[5] S.C. Kim, F.E. Massoth, J. Catal. 189 (2000) 70.
[6] R. Prins, Adv. Catal. 46 (2001) 399.
[7] F. Rota, R. Prins, J. Catal. 202 (2001) 195.
[8] M. Nagai, Y. Goto, H. Ishii, S. Omi, Appl. Catal. A: Gen. 192 (2000) 189.
[9] M. Nagai, Y. Goto, O. Uchino, S. Omi, Catal. Today 4 (1998) 249.
[10] M. Nagai, Y. Goto, A. Irisawa, S. Omi, J. Catal. 191 (2000) 128.
[11] P. Da Costa, C. Potvin, J.-M. Manoli, M. Breysse, G. Djéga-Mariadassou, Catal. Lett. 65 (2001) 195.
[12] E. Furimsky, Appl. Catal. A: Gen. 240 (2003) 1.
[13] L. Volpe, M.J. Boudart, Solid State Chem. 59 (1985) 332.
[14] L. Volpe, M.J. Boudart, Solid State Chem. 59 (1985) 348.
[15] H. Topsøe, B.S. Clausen, F.E. Massoth, Hydrotreating Catalysis – Science and Technology, 11, Springer, Berlin, 1996.
[16] B.T. Dhandapani, St. Clair, S.T. Oyama, Appl. Catal. A: Gen. 168 (1998) 219.
[17] M.J. Girgis, B.C. Gates, Ind. Eng. Chem. Res. 30 (1991) 2021.
[18] R. Shafi, G.J. Hutchings, Catal. Today 59 (2000) 423.
[19] M. Houalla, N.K. Nag, A.V. Spare, D.H. Broderick, B.C. Gates, AIChE J. 24 (1978) 1015.
[20] J. Mijoin, G. Pérot, F. Bataille, J.L. Lemberton, M. Breysse, S. Kasztelan, Catal. Lett. 71 (2001) 139.
[21] X. Duan, Y. Teng, A. Wang, V.M. Kogan, X. Li, Y. Wang, J. Catal. 261 (2009) 232.
[22] M. Boudart, G. Djéga-Mariadassou, Kinetics of Heterogeneous Catalytic Reactions", Princeton University Press, Princeton, 1984.
[23] G. Djéga-Mariadassou, M. Boudart, J. Catal. 216 (2003) 89.
[24] J.S. Choi, G. Bugli, G. Djéga-Mariadassou, J. Catal. 193 (2000) 238.
[25] R.B. Levy, M. Boudart, Science 181 (1973) 547.
[26] K. Neylon, S. Choi, H. Kwon, K.E. Curry, L.T. Thompson, Appl. Catal. A: Gen. 183 (1999) 253.
[27] A. Szymanska, M. Lewandowski, C. Sayag, G. Djega-Mariadassou, J. Catal. 218 (2003) 24.
[28] M. Lewandowski, P. Da Costa, D. Benichou, C. Sayag, Appl. Catal. B: Environ. 93 (2010) 241.
[29] S. Ramanathan, S.T. Oyama, J. Phys. Chem. 99 (1995) 16365.
[30] P.A. Aegerter, W.W.C. Quigley, G.J. Simpson, D.D. Ziegler, J.W. Logan, K.R. McCrea, S. Glazier, M.E. Bussell, J. Catal. 164 (1996) 109.
[31] K.R. McCrea, J.W. Logan, T.L. Tarbuck, J.L. Heiser, M.E. Bussell, J. Catal. 171 (1997) 255.
[32] A.S. Mamède, J.M. Giraudon, A. Löfberg, L. Leclercq, G. Leclercq, Appl. Catal. A: Gen. 227 (2002) 73.
[33] S. Korlann, B. Diaz, M.E. Bussell, Chem. Mater. 14 (2002) 4049.
[34] B. Dıaz, S.J. Sawhill, D.H. Bale, R. Main, D.C. Phillips, S. Korlann, R. Self, M.E. Bussell, Catal. Today 86 (2003) 191.
[35] W. Wu, Z. Wu, Z. Feng, P. Ying, C. Li, Phys. Chem. Chem. Phys. 6 (2004) 5596.
[36] P. Liu, J.A. Rodriguez, J.T. Muckerman, J. Mol. Catal. A: Chem. 239 (2005) 116.
[37] P. Liu, J.A. Rodriguez, T. Asakura, J. Gomes, Kenichi Nakamura, J. Phys. Chem. B 109 (2005) 4575.
[38] V. Sundaramurthy, A.K. Dalai, J. Adjaye, Catal. Today 125 (2007) 239.
[39] E. Puello-Polo, J.L. Brito, J. Mol. Catal. A: Chem. 281 (2008) 85.
[40] E. Puello-Polo, J. Brito, Catal. Today 149 (2010) 316.
[41] E. Puello-Polo, A. Gutierrez-Alejandre, G. Gonzalez, J.L. Brito, Catal. Lett. 135 (2010) 212.
[42] J.A. Rodriguez, P. Liu, Y. Takahashi, K. Nakamura, F. Illes, Top. Catal. 53 (2010) 393.
[43] J.C. Schlatter, S.T. Oyama, J.E. Metcalfe III, J.M. Lambert, Ind. Eng. Chem. Res. 27 (1988) 1648.
[44] D.J. Sajkowski, S.T. Oyama, Appl. Catal. A: Gen. 134 (1996) 339.
[45] J.S. Lee, T. Oyama, M. Boudart, J. Catal. 106 (1987) 125.
[46] M.M. Nigra, A. Katz "Molecular-Level Structure-Function Relations in Gold Nanoparticle Catalysis", November 1, 2012: 5:15 PM 319 (Convention Centre), https//aiche.confex.com/aiche/2012/webprogram/Paper280512.html.
[47] V.M. Kogan, P. l, A. Nikulshin, N.N. Rozhdestvenskaya, Fuel 100 (2012) 2.
[48] H. Wang, E. Iglesia, ChemCatChem 3 (2011) 1166.
[49] H. Wang, E. Iglesia, J. Catal. 273 (2010) 245.
[50] P. Da Costa, C. Potvin, J.-M. Manoli, J.-L. Lemberton, G. Pérot, G. Djéga-Mariadassou, J. Mol. Catal. A: Chem. 184 (2002) 323.
[51] A. Szymańska-Kolasa, M. Lewandowski, C. Sayag, G. Djéga-Mariadassou, Catal. Today 119 (2007) 7.
[52] A. Hynaux, C. Sayag, S. Suppan, J. Trawczyński, M. Lewandowski, A. Szymańska-Kolasa, G. Djéga-Mariadassou, Catal. Today 119 (2007) 3.
[53] A. Hynaux, C. Sayag, S. Suppan, J. Trawczyński, M. Lewandowski, A. Szymańska-Kolasa, G. Djéga-Mariadassou, Appl. Catal. B: Environ. 72 (2007) 62.
[54] H. Tominaga, M. Nagai, Appl. Catal. A: Gen. 389 (2010) 195.